Green Chemistry

PAPER

View Article Online
View Journal | View Issue

Cite this: *Green Chem.*, 2021, **23**, 1772

High-performance bio-based epoxies from ferulic acid and furfuryl alcohol: synthesis and properties†

Jiale Ye,[a,b] Songqi Ma, *[b] Binbo Wang,[b] Qingming Chen,[a] Kaifeng Huang,[b] Xiwei Xu,[b] Qiong Li,[b] Sheng Wang,[b] Na Lu[b] and Jin Zhu[b]

Received 20th November 2020,
Accepted 20th January 2021

DOI: 10.1039/d0gc03946b

rsc.li/greenchem

The lignin derivative ferulic acid was directly functionalized to diepoxy which could be co-cross-linked with furfuryl alcohol-derived monoepoxy to achieve high-performance bio-based thermosets. The development of high-performance bio-based epoxy as a sustainable alternative to fossil-sourced bisphenol A epoxy has great significance. In this work, ferulic acid-based diepoxy (FAE) was facilely synthesized through a direct reaction with epichlorohydrin. After cross-linking, its thermal and mechanical properties are comparable with or even higher than those of bisphenol A epoxy. The carbon–carbon double bond in the framework of the FAE was also exploited to further upgrade its properties *via* the Diels–Alder reaction with a synthesized glycidyl ether of furfuryl alcohol (GEFA). The chemical structures of FAE and GEFA, curing kinetics, and the Diels–Alder reaction were characterized in detail. The glass transition temperature of FAE-GEFA systems reached ~250 °C. This work provides a simple way to achieve high-performance thermosets from ferulic acid, and also offers a promising sustainable alternative to bisphenol A epoxy.

1. Introduction

Thermosets are three-dimensional cross-linked polymeric materials that cannot be dissolved in solvents or melted, and they have been widely used in coatings, circuit components, composite materials, *etc*. As one of the most paramount thermosets, epoxy has excellent physical and chemical properties, such as high hardness, superior wettability, oil resistance, water and corrosion resistance, and favorable insulation. Besides, it has low cross-linked curing volume shrinkage and will not lose adhesion resulting from internal stress. Owing to these excellent properties and long service life, epoxy is widely used. Nowadays, the majority of commercial epoxies are bisphenol A (BPA) epoxy (DGEBA). BPA comes from non-renewable fossil resources, and is harmful to the human body. Recent studies have demonstrated that BPA may be as effective as estradiol in triggering some receptor responses,[1] and it may act as an androgen receptor antagonist.[2,3] As a result, developing sustainable alternatives to bisphenol A epoxy has become extremely urgent and significant.

In recent years, under the tremendous pressure of environmental pollution and crude oil shortage, increasing attention has been paid to using renewable biomass to produce useful polymers and composites. Researchers from all over the world have shown great interest in developing bio-based epoxy as an alternative to bisphenol A epoxy.[4–11] For instance, Li *et al.*[12] functionalized epoxy soybean oil and synthesized epoxy soybean oil-based adhesives. However, on account of the limitation of bonding strength, they can only be applied to ordinary office products. Lukaszczyk *et al.*[13] synthesized an isosorbide-based epoxy with excellent mechanical properties comparable with those of bisphenol A epoxy, while it exhibits high water adsorption in virtue of its hydrophilicity structure, which limits its application. de Kruijf *et al.*[14] carried out electrochemical dehydrogenation and dimerization of eugenol, and then epoxidized it to obtain bio-based bisphenol epoxy with high T_g and mechanical properties, but its thermal stability is lower than that of bisphenol A epoxy. Zhang's group[15] reported a rosin-based epoxy with excellent mechanical properties and thermal stability, but it is brittle on account of the stiff structure of rosin. Tian *et al.*[16] prepared resveratrol-based epoxy with high T_g, superior mechanical properties and low flammability, which enriched the types of bio-based epoxy. Nouailhas *et al.*[17] used catechin to synthesize epoxy which exhibited comparable thermal properties to bisphenol A epoxy. Recently, Weng and coworkers[18–20] developed several high-performance bio-based epoxies containing aromatic N-heterocycle, aromatic *s*-triazine, and magnolol structures. In our previous work, we also synthesized a series of epoxies with

[a]*Faculty of Materials Science and Engineering, Kunming University of Science and Technology, Kunming 650093, China*
[b]*Key Laboratory of Bio-based Polymeric Materials Technology and Application of Zhejiang Province, Laboratory of Polymers and Composites, Ningbo Institute of Materials Technology and Engineering, Chinese Academy of Sciences, Ningbo 315201, P. R. China. E-mail: masongqi@nimte.ac.cn; Tel: +86-574-87619806*
†Electronic supplementary information (ESI) available. See DOI: 10.1039/d0gc03946b

high performance from itaconic acid[21–23] and vanillin.[24–28] However, bio-based epoxies with high performance are still limited, and more new structures with simple synthesis processes should be explored.

In this work, ferulic acid (naturally occurring phenolic acid, found in bagasse, wheat and rice bran, and beetroot pulp, can also be obtained from the depolymerization of lignin,[29,30] and has been reported as a bio-based aromatic monomer capable of functionalization[31]) and furfuryl alcohol (made from furfural extracted from various agricultural and sideline products) were used as renewable raw materials to prepare bio-based epoxy monomers. So far, ferulic acid derivatives have been successfully applied as polymer structural units for the synthesis of new copolyesters, copoly(ester-urethane)s,[32] poly(anhydride-ester)s,[33] isocyanate-based polyurethanes[34] and poly(ester-alkenamer)s,[35] and ferulic acid was also utilized to produce epoxy *via* a two-step transformation into bisferulates and a further reaction with epichlorohydrin, while their glass transition temperatures (T_gs, 32–98 °C) are much lower than those of bisphenol A epoxy (150–170 °C).[36,37] Besides, the carbon–carbon double bond in the framework of ferulic acid was neglected or wasted. Thus, in this work, ferulic acid was directly utilized to synthesize diepoxy by reacting with epichlorohydrin. The obtained ferulic acid-based epoxy exhibited higher T_g and tensile strength than bisphenol A epoxy, and its properties were further improved by introducing furfuryl alcohol-derived monoepoxy through the Diels–Alder reaction with the carbon–carbon double bond of ferulic acid (Fig. 1). The chemical structures of the epoxies, the curing process and the thermal and mechanical properties were systematically investigated.

2. Experimental

2.1. Materials

Ferulic acid (99%), furfuryl alcohol (98%), epichlorohydrin (ECH), and dimethyl diphenylsulfone (DDS, active hydrogen equivalent weight (AHEW): 124 g per N–H) were obtained from Aladdin Reagent, China. Tetrabutyl ammonium bromide (TBAB) and sodium hydroxide were supplied by Sinopharm Chemical Reagent Co., Ltd, China. Epoxy (DGEBA, trade name DER332, 172–176 g per eq.) was supplied by DOW Chemical Company. All the chemicals were used as received.

2.2. Preparation of the ferulic acid-based epoxy monomer (FAE)

20 g (0.1 mol) of ferulic acid, 120 g (1.3 mol) of ECH and 0.2 g of TBAB were placed in a 500 mL single-necked round-bottomed flask with a magnetic stirrer and a reflux condenser. After the reactants were mixed vigorously at room temperature for 5 min, the reaction mixture was heated to approximately 105 °C and maintained at this temperature for 0.5 h. Then the mixture was cooled to room temperature and 50 g of 40 wt% sodium hydroxide aqueous solution was added dropwise and the reaction mixture was kept at 0–10 °C for 3 h before being washed with deionized water five times. After removing water and residual ECH using a rotary evaporator, the obtained product was dissolved in 20 g of acetone and precipitated by being dropped into *n*-hexane, and this was repeated three times. Finally, around 18 g of FAE (yield: 60%) was obtained after filtration and drying at 60 °C for 1 h. The synthesis route is illustrated in Scheme 1.

^{1}H NMR (DMSO-d$_6$, ppm): δ = 7.63 (d, 1H), 7.41 (d, 1H), 7.25 (dd, 1H), 7.0 (d, 1H), 6.64 (d, 1H), 4.51 (dd, 1H), 4.36 (dd, 1H), 3.90 (m, 2H), 3.83 (s, 3H), 3.26 (dq, 1H), 2.84 (dt, 2H), 2.7 (td, 2H).

^{13}C NMR (DMSO-d$_6$, ppm): δ = 166.67 (s, 1C), 150.41 (s, 1C), 149.57 (s, 1C), 149.59 (s, 1C), 127.75 (s, 1C), 123.36 (s, 1C), 115.75 (s, 1C), 113.33 (s, 1C), 111.24 (s, 1C), 70.21 (s, 1C), 65.28 (s, 1C), 56.13 (s, 1C), 50.07 (s, 1C), 49.56 (s, 1C), 44.33 (s, 1C), 44.26 (s, 1C).

The molecular weight measured by TOF-MS was 226 g mol^{-1}. The epoxide equivalent weight (EEW) was found to be 113 g per eq.

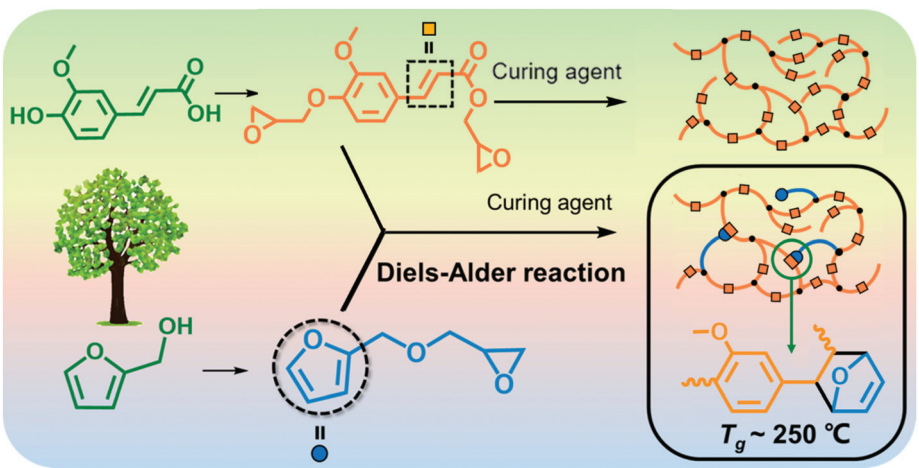

Fig. 1 Schematic diagram of the preparation of ferulic acid and furfuryl alcohol epoxies and their cross-linked networks.

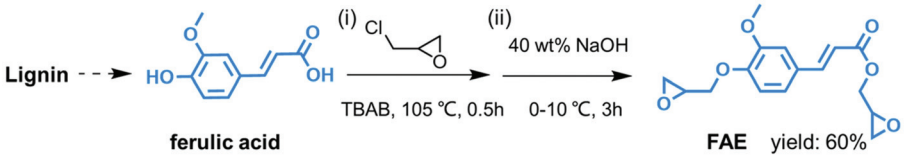

Scheme 1 Synthesis route of FAE.

2.3. Preparation of glycidyl ether of furfuryl alcohol (GEFA)

20 g (0.2 mol) of furfuryl alcohol, 120 g (1.3 mol) of ECH, 0.2 g of TBAB and 50 g of 40 wt% sodium hydroxide aqueous solution were placed in a 500 mL single-necked round-bottomed flask with a magnetic stirrer. The reaction mixture was kept at 0–10 °C for 24 h before being washed with deionized water five times. The obtained yellow liquid was distilled under reduced pressure to obtain 29 g of GEFA (yield: 90%). The synthesis route is illustrated in Scheme 2.

^{1}H NMR (DMSO-d_6, ppm): δ = 7.64 (q, 1H), 6.43 (d, 2H), 4.46 (m, 2H), 3.71 (ddt, 2H), 3.26 (m, 1H), 3.09 (dtd, 1H), 2.72 (dd, 1H), 2.54 (ddd, 1H).

^{13}C NMR (DMSO-d_6, ppm): δ = 151.87 (s, 1C), 143.60 (s, 1C), 110.87 (s, 1C), 110.03 (s, 1C), 70.90 (s, 1C), 64.51 (s, 1C), 50.61 (s, 1C), 43.87(s, 1C).

The molecular weight measured by TOF-MS was 154 g mol^{-1}. The epoxide equivalent weight (EEW) was found to be 87 g per eq.

2.4. Preparation of the FAE epoxy network

After mixing FAE and DDS at a molar ratio of 2 : 1 (the molar ratio of the epoxy group to active hydrogen is 1 : 1) and uniformly grinding them, they were melted in a stainless steel mold at 100 °C. After that, the mixture was degassed in a vacuum oven at 100 °C for at least 30 min, and then cured at 180 °C for 2 h, 200 °C for 2 h, and 220 °C for 2 h to obtain the FAE epoxy network. The DGEBA epoxy network (named DGEBA) was prepared from DGEBA and DDS (the molar ratio of the epoxy group to active hydrogen is 1 : 1) using the same curing process.

2.5. Preparation of the FAE-GEFA epoxy network

FAE, GEFA and DDS were mixed together to produce FAE-GEFA epoxy networks. The molar ratios of FAE and GEFA were kept at 1 : 0.25, 1 : 0.5 and 1 : 1 (Table 1). The molar ratio of the epoxy group from FAE and GEFA and the N–H bond from DDS was 1 : 1. They were melted in a beaker at 110 °C and stirred uniformly. After making them completely transparent, they were placed flat on a 180 °C tinplate for pre-curing for 2 h, and then placed in a vacuum oven at 200 °C and 220 °C for 2 h, respectively, to obtain the FAE-GEFA epoxy network.

Table 1 Feed compositions of the samples

Sample name		Epoxy (equiv.)		
Uncured mixture	Cured	FAE	GEFA	DGEBA
FAE_1-$GEFA_0$-DDS	FAE_1GEFA_0	1	0	0
FAE_1-$GEFA_{0.25}$-DDS	$FAE_1GEFA_{0.25}$	1	0.25	0
FAE_1-$GEFA_{0.5}$-DDS	$FAE_1GEFA_{0.5}$	1	0.5	0
FAE_1-$GEFA_1$-DDS	FAE_1GEFA_1	1	1	0
DGEBA-DDS[27]	DGEBA	0	0	1

2.6. Characterization

^{1}H NMR and ^{13}C NMR spectra were obtained using an AVANCE III Bruker NMR spectrometer (Bruker, Switzerland) operating at 400 MHz and 101 MHz, respectively, and DMSO-d_6 and $CDCl_3$ were used as solvents. TOF-MS was measured using a Triple TOF 4600 time of flight mass spectrometer (AB Sciex, America), and methylene chloride was used as the solvent. GC-MS was performed using a 7890B-5977A gas chromatography-mass spectrometer (GC-MS) (Agilent, America), methylene chloride was used as the solvent, and EI was used as the ion source. The infrared spectra (FTIR) were recorded with a Nicolet 6700 FTIR system (Nicolet, America) using the KBr pellet method. The scan range was from 500 cm^{-1} to 4000 cm^{-1} and each sample was scanned 32 times. Rheological measurements were performed using a TA HR-3 rheometer equipped with a convection oven under nitrogen using a parallel plate geometry (diameter 25 mm). Viscosity measurement was carried out at 25 °C and 80 °C by applying a constant shear rate of 5 s^{-1}. Differential scanning calorimetry (DSC) was carried out on a PerkinElmer DSC8000 system under a nitrogen atmosphere. The melting point of FAE was measured by DSC from 25 to 300 °C at a heating rate of 5 °C min^{-1}. The glass transition temperature is measured using the following steps: in the first heating step, the sample was heated to 250 °C at a rate of 10 °C min^{-1}, and kept at 220 °C

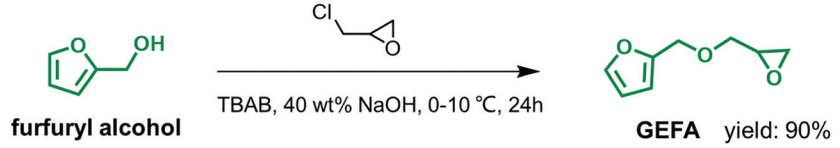

Scheme 2 Synthesis route of GEFA.

for 5 min to eliminate the thermal history, and then the temperature was cooled to 25 °C at a rate of 50 °C min^{-1}, and kept at 25 °C for another 5 min, and finally heated to 250 °C at a rate of 10 °C min^{-1} for the second heating scan. The glass transition temperature (T_g) was obtained from the peak temperature of the differential curve of the second heating curve of the cured samples. The non-isothermal curing kinetics of FAE-GEFA systems were studied by DSC, and Kissinger's method (eqn (1))[38] and Ozawa's method (eqn (2))[39] were used to calculate the apparent activation energy during the curing process.

$$-\ln\left(q/{T_p}^2\right) = E_a/RT_p + \ln\left(AR/E_a\right) \quad (1)$$

$$\ln q = -1.052 \times E_a/RT_p + \ln\left(AE_a/R\right) - \ln F(x) - 5.331 \quad (2)$$

where q is the heating rate, T_p is the peak exothermic temperature, E_a is the average activation energy of the curing reaction, A is the pre-exponential factor, R is the gas constant, and $F(x)$ is a conversion-dependent term. Thermogravimetric analysis (TGA) was performed with a Mettler-Toledo TGA/DSC thermogravimetric analyzer (Switzerland) at a heating rate of 20 °C min^{-1}, from 50 °C to 800 °C, under a nitrogen atmosphere. Dynamic mechanical analysis (DMA) was carried out on a TA Instruments Q800 DMA system in tension mode to measure the dynamic mechanical properties of the thermosetting plastics. The thermosetting plastics with dimensions of 25 mm (length) × 6 mm (width) × 1 mm (thickness) were prepared and tested from −50 °C to 300 °C at a heating rate of 3 °C min^{-1} and a frequency of 1 Hz. For the gel content measurement, four groups of the cured FAE-GEFAs (around 200 mg per group) were placed in a Soxhlet extractor and extracted with acetone for 60 h, and then taken out and placed in a vacuum oven at 60 °C for 12 h. The original mass is recorded as m, the final mass after extraction is recorded as m', and the gel content is calculated using m'/m. The theoretical cross-link density of the cured epoxy was estimated by calculating the average molecular weight between the cross-link points (M_c) using eqn (3) and (4).[26,40]

$$M_{C1} = \frac{n_{FAE} \times M_{FAE} + n_{DDS} \times M_{DDS}}{n_{DDS}} \quad (3)$$

$$M_{C2} = \frac{n_{DGEBA} \times M_{DGEBA} + n_{DDS} \times M_{DDS}}{n_{DDS}} \quad (4)$$

where n and M represent the molarity and molar mass of the corresponding component in the epoxy formulations. Meanwhile, the actual cross-link density (ν_e) of the cured epoxies was calculated using eqn (5) based on the data obtained by DMA.[41,42]

$$E' = 3\nu_e RT \quad (5)$$

where E' is the storage modulus of the samples in the rubbery plateau region at T_g +50 °C, R is the gas constant, and T is the absolute temperature.

3. Results and discussion

3.1. Synthesis and characterization of FAE and GEFA

In this work, ferulic acid-based epoxy (FAE) was synthesized *via* a heavily used two-step reaction (ring-open and ring-close) with epichlorohydrin (Scheme 1). It is worth noting that epoxidation of phenolic hydroxyl and carboxyl groups was carried out simultaneously in one pot, which manifests that there is no need to extract intermediate products during the reaction. A similar epoxidation process of gallic acid, a monomer with a phenolic hydroxyl group and carboxylic acid, was reported by Aouf *et al.*[43] They first allylated gallic acid, and then the resulting product reacted with *meta*-chloroperbenzoic acid to afford the epoxy monomer. The whole process is complicated. In contrast, our synthesis route is simple and efficient.

FTIR, ^{1}H NMR, ^{13}C NMR and TOF MS spectra were recorded to identify the chemical structure of FAE. Fig. 2a presents the ^{1}H NMR spectrum of FAE. The peaks at around 2.68 ppm, 2.84 ppm, 3.26 ppm and 3.35 ppm belong to the six protons of the two epoxy groups, and the peaks at around 3.85 ppm, 3.94 ppm, 4.37 ppm and 4.52 ppm correspond to the four protons of the –C***H***$_2$– next to the epoxy groups. The peaks at around 7.00 ppm, 7.26 ppm, and 7.41 ppm represent the three protons on the benzene ring, the peak at 3.83 ppm belongs to the three protons of the –OC***H***$_3$ on the benzene ring, and the peaks at 6.66 ppm and 7.65 ppm are ascribed to the two protons of –C***H***=C***H***– conjugated with the benzene ring. Besides, the integral areas of all the peaks are matched well with the chemical structure of FAE. With the interest of confirming the chemical structure of FAE, ^{13}C NMR, FTIR and TOF MS spectra were also recorded. Both the chemical shifts and the number of peaks in the ^{13}C NMR spectrum (Fig. 2b) are in agreement with the chemical structure of FAE; the characteristic peak of the epoxy group appears at 910 cm^{-1} in the FTIR spectrum of FAE (Fig. 2c); and the TOF MS spectrum in Fig. 2d presents a molecular ion peak of FAE at m/z 307.12, corresponding to its molecular weight of 306 g mol^{-1} for FAE. These results indicate that the target compound FAE has been successfully synthesized. Similarly, we used a similar method to synthesize glycidyl ether of furfuryl alcohol (GEFA) (Scheme 2), and its chemical characterization was also determined by ^{1}H NMR, ^{13}C NMR and GC-MS spectra (Fig. S1†). The chemical shift of proton peaks and integral area in the ^{1}H NMR spectrum (Fig. S1a†) and the number of peaks and chemical shifts in the ^{13}C NMR spectrum (Fig. S1b†) are all in agreement with the target chemical structure of GEFA. The GC-MS spectrum in Fig. S1c† presents a molecular ion peak of GEFA at m/z 154.1, corresponding to its molecular weight of 154 g mol^{-1} for GEFA.

The appearance, melting point of FAE and viscosity of the melted FAE at temperatures below the melting point are illustrated in Fig. 3. As illustrated, the melting point of FAE by DSC is 104 °C (Fig. 3a). For the most solid epoxy, their melted samples would return to the solid state immediately after cooling to the temperatures below their melting points. Interestingly, when FAE was melted from solid to liquid, its

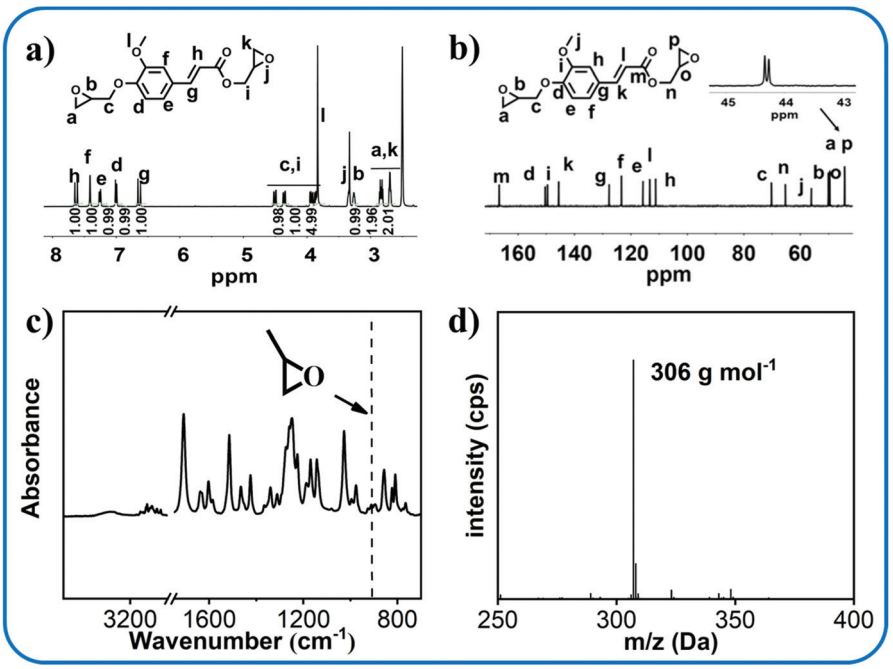

Fig. 2 (a) ^{1}H NMR, (b) ^{13}C NMR, (c) FTIR and (d) TOF MS spectra of FAE.

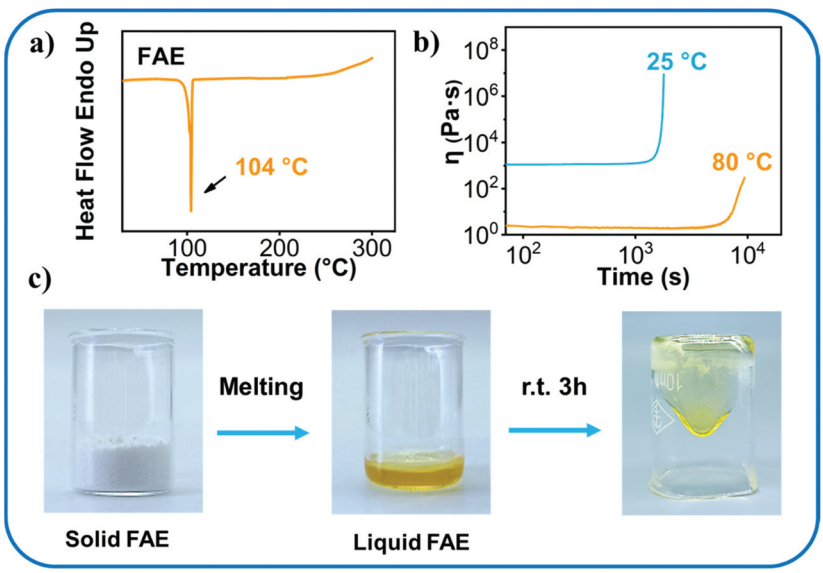

Fig. 3 (a) Melting point of FAE by DSC. (b) Viscosity as a function of time at 25 °C and 80 °C for the melted FAE by rheology. (c) Digital photos of solid and melted FAE.

liquid state would not transform into the solid state at temperatures below the melting point immediately. As can be seen in Fig. 3b, during the rheology measurement by applying a constant shear rate of 5 s^{-1}, the viscosities of the melted FAE could be kept stable for several hours before increasing to extremely high viscosities (solid state) at 80 °C and at 25 °C; and in the static state, the liquid state of FAE could be maintained at room temperature for 3 h without solidification (Fig. 3c). This property provides favorable processing performance for the preparation of epoxy composites and coatings.[9] At high temperatures above the melting point of epoxy, the reaction of the epoxy group and the curing agent could proceed quickly, and as a result, the processing time for mixing, degassing, *etc*. is short, which will limit their application. To address this issue, organic solvents were often utilized to dissolve the epoxy-curing agent systems. Although the melting point of FAE is 104 °C at which the curing reaction often proceeds extremely quickly, the mixing and degassing processes could be finished

at room temperature or lower temperatures below 104 °C because of its stable liquid state below the melting point. On account of the low viscosity of GEFA, the processability of FAE-GEFA systems was improved further.

3.2. Preparation of FAE and FAE-GEFA epoxy networks

Since the discovery of the Diels–Alder reaction in 1928, it has become one of the effective methods for synthesizing six-membered rings. Recently, many researchers have applied this reaction to the field of bio-based polymers and have made meaningful progress.[31,44,45] For example, Dello Iacono *et al.*[46] endowed the epoxy thermoset with self-healing properties through the introduction of the Diels–Alder reaction. The Diels–Alder reaction mainly occurs between electron-rich diene compounds (such as cyclopentadiene and furan derivatives, *etc.*) and electron-deficient dienophiles (such as maleimide (MI) derivatives, *etc.*) in a [4 + 2] cycloaddition reaction to form a stable six-membered ring compound. The Diels–Alder reaction generally has the advantages of mild conditions, without adding catalysts, *etc.* During the process of preparing the FAE-GEFA networks, the Diels–Alder reaction would occur due to the presence of the cyclic diene of the furan ring and the carbon–carbon double bond in FAE, as shown in Fig. 4. The curing of FAE and DDS results in a FAE network, as presented in Fig. S2.†

In order to verify whether the Diels–Alder reaction is indeed proceeding smoothly as expected, we protected the phenolic hydroxyl and carboxyl groups of ferulic acid (named *P*-FAE and the ^{1}H NMR of *P*-FAE is shown in Fig. S3†), and then performed a small-molecule model reaction with GEFA. As shown in Fig. 5 and Fig. S3,† *P*-FAE, GEFA and their mixture were heated at 140 °C for 6 h, and then subjected to ^{1}H NMR spectroscopy. Obvious differences were found. It can be seen that the treated mixture exhibited obvious characteristic peaks of DA adducts at 5.3 ppm, 5.1 ppm and 4.8 ppm (two isomeric products existed). The extent of the DA reaction calculated by the integral area is around 80%, which manifests that the DA reaction can proceed as expected during the curing process. The obtained mixture from the above reaction of *p*-FAE + GEFA

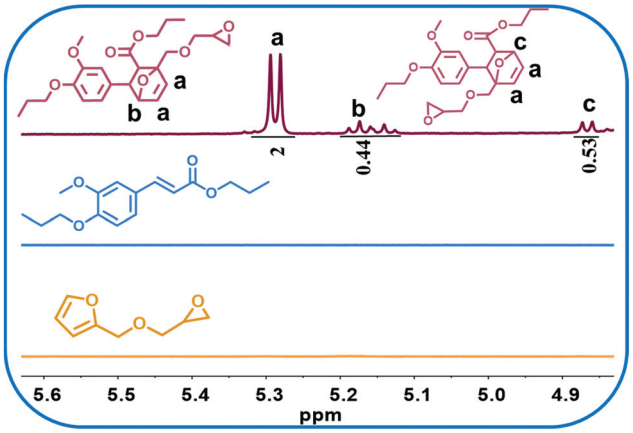

Fig. 5 ^{1}H NMR spectra of *P*-FAE, GEFA and *p*-FAE + GEFA reacted at 140 °C for 6 h.

was further heated at 200 °C for 2 h, and the peak strength for the DA adducts did not decrease (Fig. S4†). This suggests that the retro-Diels–Alder reaction is difficult to proceed for these DA adducts.

The non-isothermal curing kinetics of FAE-GEFA systems were studied by DSC. According to Kissinger's method (eqn (1)) and Ozawa's method (eqn (2)), the lower T_p and E_a often signify a better chance for the curing reaction to take place and a higher reactivity under the same curing conditions. Taking FAE_1GEFA_0 as an example, we conducted a non-isothermal DSC test with four different heating rates, and the results are illustrated in Fig. 6a. The exothermic peaks at around 100 °C are mainly attributed to the melting of FAE in the mixtures before curing. The endothermic peaks at around 180–220 °C belong to the curing of the mixtures. Fig. 6b and c shows the relationship between $-\ln(q/T_p^2)$ and $1/T_p$ based on Kissinger's method, and the relationship between $\ln q$ and $1/T_p$ based on Ozawa's method for FAE-GEFA systems, and Table 2 summarizes the E_as calculated from the slope of the linear fitting curve. It can be seen that FAE-GEFA-DDS systems exhibit similar E_a values to DGEBA-DDS systems, which

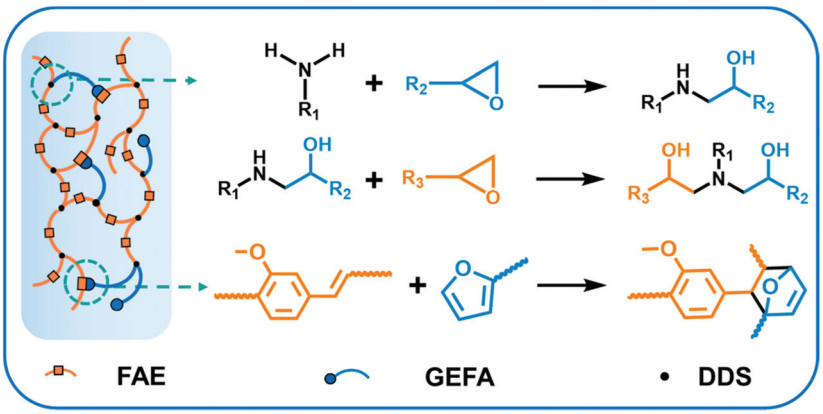

Fig. 4 Reactions during the preparation of FAE-GEFA epoxy networks.

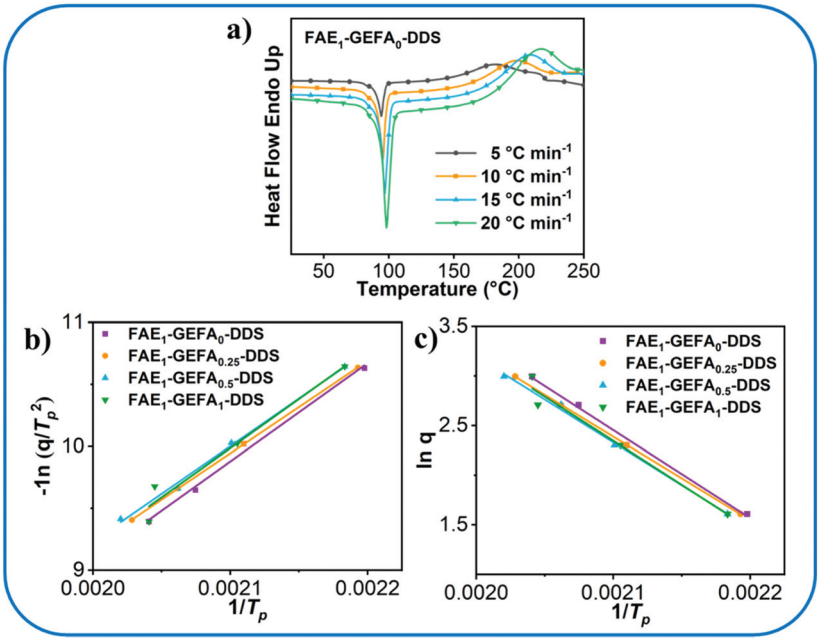

Fig. 6 (a) Non-isothermal DSC curves of the FAE-GEFA-DDS system at different heating rates. Linear plots of (b) $-\ln(q/T_p^2)$ *versus* $1/T_p$ based on Kissinger's equation and (c) ln q *versus* $1/T_p$ based on Ozawa's theory.

Table 2 Peak temperatures of the non-isothermal DSC curves of different curing systems at different heating rates and their activation energies (E_as)

	T_p under different heating rates (°C)				E_a (kJ mol^{-1})	
Sample	5 °C min^{-1}	10 °C min^{-1}	15 °C min^{-1}	20 °C min^{-1}	Kissinger	Ozawa
FAE_1-$GEFA_0$-DDS	182	201	209	217	66.0	70.2
FAE_1-$GEFA_{0.25}$-DDS	183	201	212	220	62.1	66.5
FAE_1-$GEFA_{0.5}$-DDS	185	203	212	222	63.9	68.2
FAE_1-$GEFA_1$-DDS	185	202	216	217	65.9	70.2
DGEBA-DDS[27]	208.6	230.5	239.6	252.3	59.8	66.5

demonstrates that the reactivity of FAE toward DDS is comparable to that of DGEBA.[27]

Based on the results of curing kinetics, the preferred curing condition of 180 °C for 2 h, 200 °C for 2 h, and 220 °C for 2 h was utilized to prepare the samples, and the appearance of the samples is shown in Fig. 7a. For the sake of investigating the curing degree of systems, the FTIR spectrum of the cured FAE_1GEFA_1 was examined and compared with that of the uncured system, as shown in Fig. 7b. Obviously, after curing, the peak of the epoxy group at 910 cm^{-1} disappeared, and a broad peak from 3200 to 3600 cm^{-1} appeared. A similar result was obtained from the FTIR spectra of the FAE_1GEFA_0 system before and after curing (Fig. S5†). Fig. 7c presents the non-isothermal DSC curves of the FAE_1GEFA_1 system before and after curing. There is an obvious exothermic peak during the curing process, but there is no visible exothermic peak for the cured sample. The gel contents of the cured samples were also measured by Soxhlet extraction for 60 h using acetone as the solvent. As can be seen from Fig. 7d, the gel contents of all samples exceed 98%. These results are indicative of the high curing degree of all the cured samples.

3.3. Glass transition temperature of the cured epoxy

The glass transition temperature (T_g) is the main parameter of thermosetting materials. The T_gs of DGEBA and FAE-GEFA networks were measured by DMA and DSC, and the results are summarized in Fig. 8a, b and Table 3.

The T_αs of FAE-GEFA networks obtained from the DMA curves (Fig. 8a) are 209 °C, 224 °C, 241 °C, and 250 °C with an increase in the content of GEFA, which are up to 56 °C higher than that of DGEBA (194 °C). The T_gs obtained from the DSC curves (Fig. 8b) show the same trend. The T_g of a cross-linked polymer is closely related to its cross-link density and the rigidity of the segment structure. The higher the cross-link density of the cross-linked polymer and the greater the rigidity of the segment, the higher the T_g.[47,48] According to eqn (3) and (4), the M_cs of the networks FAE_1GEFA_0 and DGEBA were found to be 860 and 928, which means that FAE_1GEFA_0 should possess

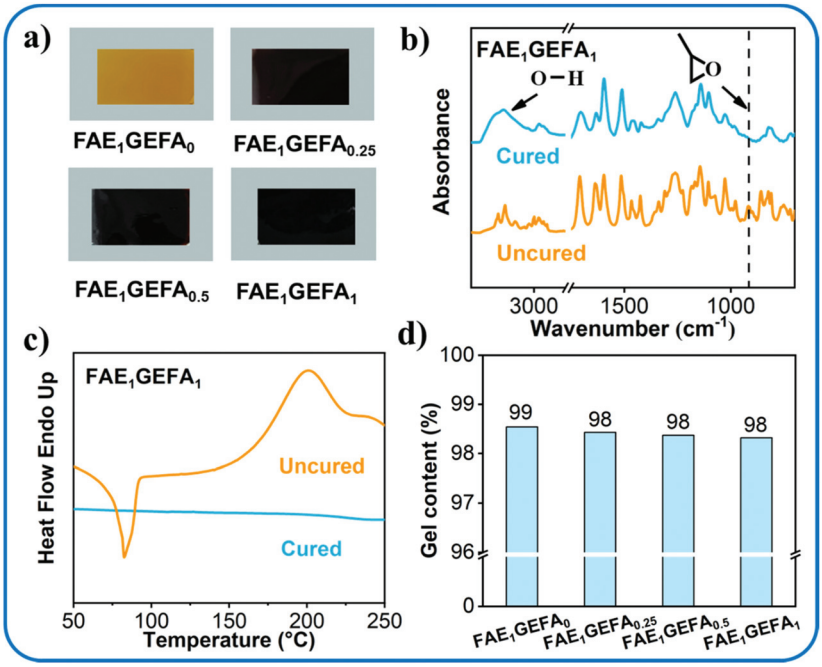

Fig. 7 (a) Digital photos of FAE-GEFAs. (b) FTIR spectra and (c) non-isothermal DSC curves of the FAE_1GEFA_1 system before and after curing. (d) Gel contents of all the cured samples.

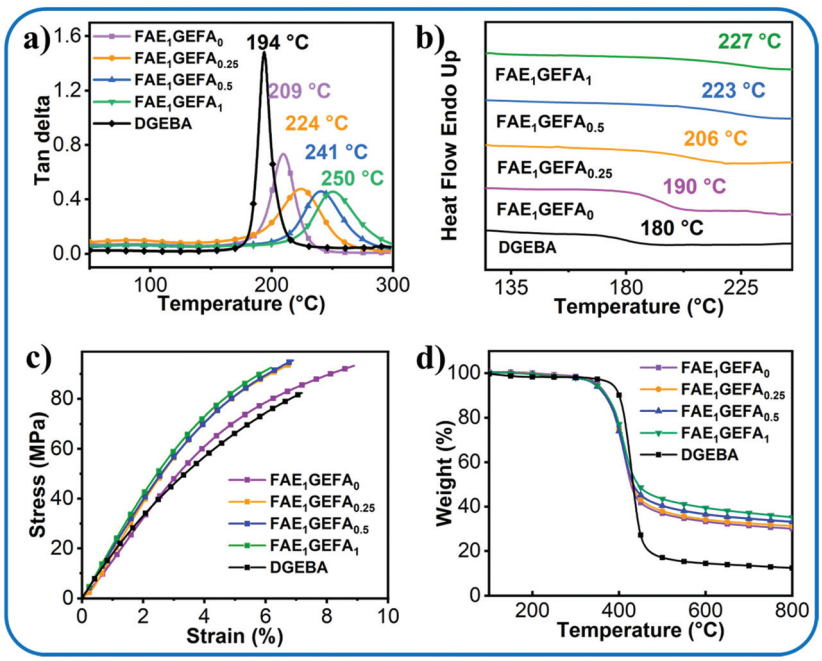

Fig. 8 (a) DMA curves, (b) non-isothermal DSC curves, (c) representative stress–strain curves, and (d) TGA curves under a nitrogen atmosphere of the cured epoxy.

a higher cross-link density than the DGEBA network. According to the relationship of the storage modulus (Fig. S6†), the values of ν_e calculated using formula (5) are summarized in Table 3. Obviously, the cross-link density of FAE_1GEFA_0 is higher than that of DGEBA, which is consistent with the theoretical M_c results. With the addition of GEFA, the formation of a Diels–Alder adduct further increases the cross-link density of the networks and the rigidity of the segments, leading to an increase in T_g. Therefore, the higher cross-link density of FAE-GEFA networks leads to higher T_gs than that of

Table 3 Glass transition temperature (T_g), storage modulus (E') at T_g +50 °C, cross-link density (ν_e) and residual carbon rate values of the cured epoxy

Sample	T_g by DSC (°C)	T_α by DMA (°C)	E' at T_g +50 °C (MPa)	ν_e (mol m^{-3})
FAE_1GEFA_0	190	209	25.2	1899
$FAE_1GEFA_{0.25}$	206	224	45.4	3327
$FAE_1GEFA_{0.5}$	223	241	52.4	3731
FAE_1GEFA_1	227	250	47.3	3309
DGEBA	180	194	18.5	1588

the DGEBA network. The cross-link density of FAE_1GEFA_1 is lower than that of $FAE_1GEFA_{0.5}$, which might be due to the fact that the Diels–Alder reaction cannot completely proceed, and the unreacted furan structure consumed the epoxy group but was not cross-linked during the curing process. In addition, there should be a more rigid Diels–Alder adduct in the network of FAE_1GEFA_1 which prevents the segment mobility, and as a result, the T_g of FAE_1GEFA_1 is higher than that of $FAE_1GEFA_{0.5}$.

3.4. Mechanical properties of the cured epoxy

Fig. 8c presents the reprehensive tensile stress–strain curves of the cured epoxies, and their tensile properties are summarized in Table 4. All of the epoxy systems exhibited tensile behaviors without a yield point. Obviously, FAE_1GEFA_0 and DGEBA are close in terms of tensile modulus, but in terms of strength, the former is 10.8 MPa higher than the latter. This is mainly because the former has higher toughness than the latter, which can be verified using the elongation at break. With the introduction of GEFA, the tensile strength of the cured epoxy showed little change, but there is a significant increase in the tensile modulus from 1710 MPa to 2298 MPa (with an increase rate of 35%). This is mainly attributed to the fact that the introduction of a Diels–Alder adduct increases the cross-link density and the rigidity of the entire network,[48] which is in agreement with the T_g result. This can also be verified from the negative correlation between the elongation at break and the addition content of GEFA.

3.5. Thermal stability of the cured epoxy

The TGA curves of the cured epoxy under a N_2 atmosphere are shown in Fig. 8d, and the data are summarized in Table 5. All the FAE-GEFA networks show similar initial degradation temperatures (the temperature for 5% weight loss, $T_{d\ 5\%}$) and temperatures for 30% weight loss ($T_{d\ 30\%}$) which are basically stable at around 350 °C and 407 °C. Due to the easy-to-detach methoxy group on the benzene ring, they started to lose weight at a lower temperature than the DGEBA network,[49] while they can still meet the general work requirements. Interestingly, the FAE-GEFA networks exhibited a much higher residual carbon rate at 800 °C (R_{800}) than the DGEBA network, and with an increase of the GEFA content, R_{800} exhibited a positive growth trend from 30% to 35%. This indicates that the benzene ring conjugated with a carbon–carbon double bond from the ferulic acid segment and the Diels–Alder adduct both are beneficial for carbonization during thermal degradation.

Table 4 Mechanical properties of the cured epoxy

Sample	Tensile strength (MPa)	Tensile modulus (MPa)	Elongation at break (%)
FAE_1GEFA_0	93.3	1710	10.0 ± 0.7
$FAE_1GEFA_{0.25}$	93.9	2176	7.2 ± 0.1
$FAE_1GEFA_{0.5}$	95.5	2298	6.4 ± 0.6
FAE_1GEFA_1	92.6	2268	6.0 ± 0.2
DGEBA	82.5	1820	7.1 ± 0.4

Table 5 Thermal stability of the cured epoxy

Sample	$T_{d\ 5\%}$ (°C)	$T_{d\ 30\%}$ (°C)	R_{800} (%)
FAE_1GEFA_0	350	407	30.1
$FAE_1GEFA_{0.25}$	350	406	31.3
$FAE_1GEFA_{0.5}$	344	405	33.2
FAE_1GEFA_1	346	409	35.2
DGEBA	384	420	12.3

4. Conclusions

A novel bio-based diepoxy was facilely synthesized from the lignin derivative ferulic acid. It possessed similar reactivity to bisphenol A epoxy, and could maintain its liquid state at room temperature for several hours after melting, which is conducive to its processing. For the first time, the carbon–carbon double bond of ferulic acid was exploited to improve the properties of its polymers. Furfuryl alcohol-derived monoepoxy was co-cross-linked with ferulic acid-derived diepoxy, and the Diels–Alder reaction occurred, which provided extra rigid cross-links for the epoxy networks, corresponding to a much higher T_g (~250 °C), tensile strength (~95.5 MPa) and modulus (~2298 MPa) than those of the bisphenol A epoxy network. Moreover, varying properties of the epoxy network could be readily achieved by adjusting the addition content of furfuryl alcohol-derived monoepoxy. This work provides a simple method to achieve high-performance bio-based epoxy with superior processability.

Conflicts of interest

There are no conflicts to declare.

Acknowledgements

The authors are grateful for the financial support from the National Natural Science Foundation of China (No. 52073296 and 51773216), the Research Project of Technology Application for Public Welfare of Ningbo City (No. 202002N3091), and the Youth Innovation Promotion Association, CAS (No. 2018335).

References

1 R. W. Stahlhut, W. V. Welshons and S. H. Swan, *Environ. Health Perspect.*, 2009, **117**, 784–789.
2 P. Roy, H. Salminen, P. Koskimies, J. Simola, A. Smeds, P. Saukko and I. T. Huhtaniemi, *J. Steroid Biochem.*, 2004, **88**, 157–166.
3 R. Urbatzka, A. V. Cauwenberge, S. Maggioni, L. Vigano, A. Mandich, E. Benfenati, I. Lutz and W. Kloas, *Chemosphere*, 2007, **67**, 1080–1087.
4 R. Auvergne, S. Caillol, G. David, B. Boutevin and J.-P. Pascault, *Chem. Rev.*, 2014, **114**, 1082–1115.
5 M. Fache, R. Auvergne, B. Boutevin and S. Caillol, *Eur. Polym. J.*, 2015, **67**, 527–538.
6 M. Fache, A. Viola, R. Auvergne, B. Boutevin and S. Caillol, *Eur. Polym. J.*, 2015, **68**, 526–535.
7 Y. Tao, L. Fang, M. Dai, C. Wang, J. Sun and Q. Fang, *Polym. Chem.*, 2020, **11**, 4500–4506.
8 T. Liu, C. Hao, L. Wang, Y. Li, W. Liu, J. Xin and J. Zhang, *Macromolecules*, 2017, **50**, 8588–8597.
9 T. Liu, C. Hao, S. Zhang, X. Yang, L. Wang, J. Han, Y. Li, J. Xin and J. Zhang, *Macromolecules*, 2018, **51**, 5577–5585.
10 F. Hu, J. J. La Scala, J. M. Sadler and G. R. Palmese, *Macromolecules*, 2014, **47**, 3332–3342.
11 S. Nameer, D. B. Larsen, J. O. Duus, A. E. Daugaard and M. Johansson, *ACS Sustainable Chem. Eng.*, 2018, **6**, 9442–9450.
12 A. Li and K. Li, *ACS Sustainable Chem. Eng.*, 2014, **2**, 2090–2096.
13 J. Lukaszczyk, B. Janicki and M. Kaczmarek, *Eur. Polym. J.*, 2011, **47**, 1601–1606.
14 G. H. M. de Kruijff, T. Goschler, N. Beiser, A. Stenglein, O. M. Tuerk and S. R. Waldvogel, *Green Chem.*, 2019, **21**, 4815–4823.
15 X. Liu and J. Zhang, *Polym. Int.*, 2010, **59**, 607–609.
16 Y. Tian, Q. Wang, L. Shen, Z. Cui, L. Kou, J. Cheng and J. Zhang, *Chem. Eng. J.*, 2020, **383**, 123124.
17 H. Nouailhas, C. Aouf, C. Le Guerneve, S. Caillol, B. Boutevin and H. Fulcrand, *J. Polym. Sci., Part A: Polym. Chem.*, 2011, **49**, 2261–2270.
18 Y. Qi, J. Wang, Y. Kou, H. Pang, S. Zhang, N. Li, C. Liu, Z. Weng and X. Jian, *Nat. Commun.*, 2019, **10**, 2107.
19 Y. Qi, Z. Weng, Y. Kou, L. Song, J. Li, J. Wang, S. Zhang, C. Liu and X. Jian, *Chem. Eng. J.*, 2021, **406**, 126881.
20 Y. Qi, Z. Weng, K. Zhang, J. Wang, S. Zhang, C. Liu and X. Jian, *Chem. Eng. J.*, 2020, **387**, 124115.
21 S. Ma, X. Liu, L. Fan, Y. Jiang, L. Cao, Z. Tang and J. Zhu, *ChemSusChem*, 2014, **7**, 555–562.
22 S. Ma, X. Liu, Y. Jiang, Z. Tang, C. Zhang and J. Zhu, *Green Chem.*, 2013, **15**, 245–254.
23 S. Ma, X. Liu, Y. Jiang, L. Fan, J. Feng and J. Zhu, *Sci. China: Chem.*, 2014, **57**, 379–388.
24 S. Ma, J. Wei, Z. Jia, T. Yu, W. Yuan, Q. Li, S. Wang, S. You, R. Liu and J. Zhu, *J. Mater. Chem. A*, 2019, **7**, 1233–1243.
25 B. Wang, S. Ma, Q. Li, H. Zhang, J. Liu, R. Wang, Z. Chen, X. Xu, S. Wang, N. Lu, Y. Liu, S. Yan and J. Zhu, *Green Chem.*, 2020, **22**, 1275–1290.
26 S. Wang, S. Ma, C. Xu, Y. Liu, J. Dai, Z. Wang, X. Liu, J. Chen, X. Shen and J. Wei, *Macromolecules*, 2017, **50**, 1892–1901.
27 W. Yuan, S. Ma, S. Wang, Q. Li, B. Wang, X. Xu, K. Huang, J. Chen, S. You and J. Zhu, *Eur. Polym. J.*, 2019, **117**, 200–207.
28 X. Xu, S. Ma, S. Wang, J. Wu, Q. Li, N. Lu, Y. Liu, J. Yang, J. Feng and J. Zhu, *J. Mater. Chem. A*, 2020, **8**, 11261–11274.
29 Y. Song, A. H. Motagamwala, S. D. Karlen, J. A. Dumesic, J. Ralph, J. K. Mobley and M. Crocker, *Green Chem.*, 2019, **21**, 3940–3947.
30 S. Wang, W. Gao, H. Li, L.-P. Xiao, R.-C. Sun and G. Song, *ChemSusChem*, 2018, **11**, 2114–2123.
31 F. Ng, G. Couture, C. Philippe, B. Boutevin and S. Caillol, *Molecules*, 2017, **22**, 149.
32 F. Pion, A. F. Reano, M. Z. Oulame, I. Barbara, A. L. Flourat, P.-H. Ducrot and F. Allais, in *Green Polymer Chemistry: Biobased Materials and Biocatalysis*, ACS Publications, 2015, pp. 41–68.
33 M. A. Ouimet, J. J. Faig, W. Yu and K. E. Uhrich, *Biomacromolecules*, 2015, **16**, 2911–2919.
34 M. Z. Oulame, F. Pion, S. Allauddin, K. V. Raju, P.-H. Ducrot and F. Allais, *Eur. Polym. J.*, 2015, **63**, 186–193.
35 I. Barbara, A. L. Flourat and F. Allais, *Eur. Polym. J.*, 2015, **62**, 236–243.
36 A. Maiorana, A. F. Reano, R. Centore, M. Grimaldi, P. Balaguer, F. Allais and R. A. Gross, *Green Chem.*, 2016, **18**, 4961–4973.
37 R. Ménard, S. Caillol and F. Allais, *Ind. Crops Prod.*, 2017, **95**, 83–95.
38 H. E. Kissinger, *J. Res. Natl. Bur. Stand.*, 1956, **57**, 217–221.
39 T. Ozawa, *J. Therm. Anal.*, 1976, **9**, 369–373.
40 T. Xie and I. A. Rousseau, *Polymer*, 2009, **50**, 1852–1856.
41 L. W. Hill, *Prog. Org. Coat.*, 1997, **31**, 235–243.
42 J. Scanlan, *J. Polym. Sci.*, 1960, **43**, 501–508.
43 C. Aouf, H. Nouailhas, M. Fache, S. Caillol, B. Boutevin and H. Fulcrand, *Eur. Polym. J.*, 2013, **49**, 1185–1195.
44 A. Duval, G. Couture, S. Caillol and L. Avérous, *ACS Sustainable Chem. Eng.*, 2016, **5**, 1199–1207.
45 A. Gandini, A. J. F. Carvalho, E. Trovatti, R. K. Kramer and T. M. Lacerda, *Eur. J. Lipid Sci. Technol.*, 2018, **120**, 1700091.
46 S. Dello Iacono, A. Martone, A. Pastore, G. Filippone, D. Acierno, M. Zarrelli, M. Giordano and E. Amendola, *Polym. Eng. Sci.*, 2017, **57**, 674–679.
47 S. Ma, D. C. Webster and F. Jabeen, *Macromolecules*, 2016, **49**, 3780–3788.
48 S. Ma and D. C. Webster, *Macromolecules*, 2015, **48**, 7127–7137.
49 J. R. Mauck, S. K. Yadav, J. M. Sadler, J. J. La Scala, G. R. Palmese, K. M. Schmalbach and J. F. Stanzione, *Macromol. Chem. Phys.*, 2017, **218**, 1700013.